

Increased Hepatic Insulin Sensitivity in Mice Lacking Inhibitory Leptin Receptor Signals

Robby Zachariah Tom, Rasmus J. O. Sjögren, Elaine Vieira, Stephan Glund, Eduardo Iglesias-Gutiérrez, Pablo M. Garcia-Roves, Martin G. Myers Jr., and Marie Björnholm

Departments of Molecular Medicine and Surgery (R.Z.T., R.J.O.S., E.V., S.G., E.I.-G., M.B.) and Physiology and Pharmacology (P.M.G.-R.), Integrative Physiology, Karolinska Institutet, SE-171 77 Stockholm, Sweden; and Department of Medicine (M.G.M.), University of Michigan, Ann Arbor, Michigan 48109

Leptin regulates food intake and energy expenditure by activating the long form of the leptin receptor (LepRb). Leptin also regulates glucose homeostasis by improving whole-body insulin sensitivity, but the mechanism remains undefined. Leptin action is mediated by phosphorylation of several tyrosine residues on LepRb. LepRb-Tyr985 plays an important role in the attenuation of LepRb signaling. We determined the contribution of LepRb-Tyr985-mediated signals to leptin action on insulin sensitivity using LepRb-Tyr985 mutant mice (*///* mice). Glucose tolerance and whole-body insulin-mediated glucose utilization were determined in wild-type (*+/+*) and *///* mice. Glucose tolerance was unaltered between female *+/+* and *///* mice but enhanced in the male *///* mice. Serum insulin concentration was decreased at baseline and 15 min after a glucose injection in female *///* vs. *+/+* mice ($P < 0.05$) but unaltered in the male *///* mice. However, basal and insulin-stimulated glucose transport in isolated soleus and extensor digitorum longus muscle was similar between *+/+* and *///* mice, indicating skeletal muscle insulin sensitivity *in vitro* was not enhanced. Moreover, euglycemic-hyperinsulinemic clamps reveal hepatic, rather than peripheral, insulin sensitivity is enhanced in female *///* mice, whereas male *///* mice display both improved hepatic and peripheral insulin sensitivity. In conclusion, signals emanating from leptin receptor Tyr985 control hepatic insulin sensitivity in both female and male *///* mice. Lack of LepRb-Tyr985 signaling enhances whole-body insulin sensitivity partly through increased insulin action on the suppression of hepatic glucose production. (*Endocrinology* 152: 2237–2246, 2011)

The adipose-derived hormone leptin regulates food intake and energy expenditure. Furthermore, leptin deficiency leads to obesity, infertility and other symptoms of neuroendocrine failure as well as insulin resistance and type 2 diabetes as described in humans and obese mouse models [*ob/ob* mice (lacking leptin) or *db/db* mice (lacking the leptin receptor)] (1–5).

Leptin can regulate glucose homeostasis indirectly, by modifying the level of adiposity, or directly, by improving insulin sensitivity. The mechanism by which leptin regulates whole-body insulin sensitivity is incompletely resolved. Leptin administration to leptin-deficient *ob/ob*

mice improves glycemic control before any effect on food intake or adiposity is observed (6), indicating that changes in insulin sensitivity are uncoupled from alterations in energy homeostasis. Leptin also enhances insulin action to inhibit hepatic glucose production (7). Central administration of either leptin or insulin suppresses glucose production, independent of changes in circulating levels of insulin (8, 9), possibly through activation of ATP-sensitive potassium channels in the hypothalamus (10). Leptin regulates lipid metabolism by increasing skeletal muscle fatty acid oxidation via activation of the energy sensor AMP-activated protein kinase (11, 12). Thus, leptin has major

ISSN Print 0013-7227 ISSN Online 1945-7170

Printed in U.S.A.

Copyright © 2011 by The Endocrine Society

doi: 10.1210/en.2010-0040 Received January 11, 2010. Accepted March 25, 2011.

First Published Online April 26, 2011

Abbreviations: EDL, Extensor digitorum longus; GSK, glycogen synthase kinase; IRS, insulin receptor substrate; Jak, Janus kinase; LepRb, long form of the leptin receptor; *///*, LepRb-Tyr985Leu; PEPCK, phosphoenolpyruvate carboxykinase 1; SCD-1, stearoyl-coenzyme A desaturase 1; SHP, Src homology-containing tyrosine phosphatase; SOCS3, suppressor of cytokine signaling 3; STAT, signal transducer and activator of transcription; tPAI, total plasminogen activator inhibitor.

effects on hepatic and peripheral metabolism through direct action at the level of these organs and indirect action via hypothalamic activation of the nervous system.

Leptin binding to the long form of the leptin receptor (LepRb), expressed primarily in the hypothalamus, results in phosphorylation of tyrosine sites on the intracellular domain of the receptor and its associated Janus kinase (Jak) 2. Three tyrosine residues on LepRb are phosphorylated upon leptin stimulation; Tyr985, Tyr1077, and Tyr1138 (13, 14). Phosphorylation of Tyr1138 of LepRb recruits the transcription factor signal transducer and activator of transcription (STAT)-3 (15, 16), which leads to the accumulation of the suppressor of cytokine signaling 3 (SOCS3) (14, 17). Leptin-mediated signals by LepRb-STAT3 are important for food intake and energy expenditure, whereas Tyr1138-independent signals are important for glucose homeostasis, growth, and reproduction (17–19). LepRb-Tyr1077 is involved in the activation of STAT5 (20). Other pathways, such as the phosphatidylinositol 3-kinase pathway, also originate directly from Jak2 (21, 22). Phosphorylation of Tyr985 recruits the Src homology containing tyrosine phosphatase (SHP)-2 to the LepRb and mediates the majority of ERK activation and c-fos transcription (14, 15). SOCS3 mediates feedback inhibition of leptin receptor signaling by binding to Tyr985 (23). We have previously disrupted the LepRb-SHP2/SOCS3 pathway in mice by mutating Tyr985 of LepRb (*l/l* mice) (24). Although growth and reproductive function are normal in *l/l* mice, body fat is decreased in female *l/l* mice, consistent with the view of inhibitory signals emanating from Tyr985 of LepRb increase leptin action. We have also shown that insulin levels in fed female mice are profoundly reduced by mutating Tyr985 of LepRb, suggesting this site also controls insulin sensitivity. We have further reported that male *l/l* mice have similar body weight and insulin levels compared with *+/+* mice. Leptin levels are, however, decreased despite a similar degree of adiposity in the male *l/l* mice.

The mechanism by which leptin enhances insulin sensitivity is incompletely understood. Thus, our aim was to investigate the signaling pathways involved in the metabolic actions of leptin. We used *l/l* mice to interrogate inhibitory signaling pathways emanating directly from the leptin receptor. We determined whether leptin receptor signaling alters peripheral or hepatic insulin sensitivity and whether LepRb-Tyr985 plays a direct role in whole-body glucose homeostasis.

Materials and Methods

Animals

Animal experiments were approved by the regional animal ethical committee. Three- to 4-month-old female and male *+/+*

and *l/l* (*Lep^r^{tm2Mgmi/tm2Mgmi}*) mice were used (24). Animals were maintained in a temperature- and light-controlled environment (12-h light, 12-h dark cycle) and had free access to water and standard rodent chow. Experiments performed in female mice were not timed to a specific phase of the estrous cycle.

Glucose tolerance test

Glucose (2 g/kg body weight) was administered to 4-h-fasted *+/+* and *l/l* mice by ip injection for the assessment of glucose tolerance. Blood glucose concentration was measured before the glucose injection and 15, 30, 60, and 120 min thereafter (One Touch Ultra glucose meter; Lifescan, Milpitas, CA). Blood samples were obtained from the tail before the glucose injection and 15 min thereafter for determination of insulin concentration using an ultrasensitive insulin ELISA kit (Crystal Chem Inc., Downers Grove, IL).

Muscle incubation procedure and blood collection

Mice were fasted for 4 h. Extensor digitorum longus (EDL) and soleus muscles were removed from anesthetized mice (avertin, 2,2,2-tribromo ethanol and tertiary amyl alcohol at 16 μ l/g body weight, ip), and *in vitro* 2-deoxyglucose transport was assessed as previously described (25). Muscles were incubated without or with insulin (0.36 and 60 nmol/liter) as indicated. After incubation, muscles were harvested, washed in ice-cold Krebs-Henseleit buffer, blotted on filter paper, and quickly frozen in liquid nitrogen and stored at -80°C . Blood was collected from the same cohort of mice for the analysis of insulin, leptin, resistin, serum monocyte chemotactic protein-1, total plasminogen activator inhibitor (tPAI)-1, TNF α , and IL-6 using a LINCOplex (Linco Research, St. Charles, MO) mouse adipokine kit, according to the manufacturer's instructions. The concentrations of monocyte chemotactic protein-1, TNF α , and IL-6 were below the detection limit of the kit in *+/+* mice. Serum adiponectin was analyzed in female *l/l* mice using a kit from R&D Systems (Minneapolis, MN).

Euglycemic-hyperinsulinemic clamp in conscious mice

Glucose turnover rate and hepatic glucose production were determined as previously described (26). Glucose turnover rate was measured in the basal state and during euglycemic-hyperinsulinemic conditions, using a constant infusion of [$3\text{-}^3\text{H}$]glucose (2.5 μCi bolus and a flow rate of 0.09 $\mu\text{Ci}/\text{min}$). Basal glucose production and utilization were assessed 65–75 min after the start of the tracer infusion. At 75 min, a euglycemic-hyperinsulinemic clamp was started. A priming dose of insulin (female mice 12.5 mU/kg; male mice 25 mU/kg) was administered, followed by a constant infusion of insulin (female mice: infusion rate 1.25 mU/kg \cdot min and male mice: infusion rate 2.5 mU/kg \cdot min). At steady state, (\sim 75 min after the start of the insulin infusion), blood samples were taken to measure whole-body glucose utilization and hepatic glucose production. Hepatic glucose production was determined by subtracting the average glucose infusion rate from the glucose utilization. Animals were euthanized by an overdose of sodium pentobarbital. Blood samples were collected to determine the insulin concentration during the clamp (ultrasensitive insulin ELISA kit; Crystal Chem). Liver was collected and immediately frozen in liquid nitrogen for analysis of insulin signaling. In a separate cohort of female mice, the insulin infusion was terminated after 10 min, and liver was dis-

sected for analysis of insulin signaling. Initial clamps in male mice with a 1.25 mU/kg · min insulin infusion rate suggested a greater hepatic insulin resistance in male compared with female mice. Therefore, male mice were clamped at a higher infusion rate (2.5 mU/kg · min) than the female mice.

In vivo insulin signaling

Mice (+/+ and *l/l*) were fasted for 4 h and then injected with insulin (0.25 mU/kg, ip). In a separate cohort, mice were injected with saline or 0.1 mU/g insulin. After 10 min, mice were euthanized with CO₂ and liver was dissected and immediately frozen in liquid nitrogen.

Tissue preparation

Muscle and liver were homogenized in ice-cold buffer [137 mmol/liter NaCl, 20 mmol/liter Tris (pH 7.8), 2.7 mmol/liter KCl, 10% glycerol, 5 mmol/liter sodium pyrophosphate, 1% Triton X-100, 1 mmol/liter MgCl₂, 10 mmol/liter sodium fluoride, 1 mmol/liter EDTA, 0.2 mmol/liter phenylmethylsulfonyl fluoride, 1 μg/ml aprotinin, 1 μg/ml leupeptin, 0.5 mmol/liter Na₃VO₄]. Homogenates were rotated end over end for 1 h at 4 C and then subjected to centrifugation (12,000 × g for 15 min at 4 C), and the supernatant was collected. Protein content in the supernatant was measured using the bicinchoninic acid method (Pierce, Rockford, IL).

Immunoblot analysis

Muscle and liver lysates were adjusted to equal protein concentration and heated in Laemmli buffer. Samples for insulin receptor and insulin receptor substrate (IRS)-1 tyrosine phosphorylation were immunoprecipitated with phosphotyrosine antibody and Dynabeads Protein A (Invitrogen, Carlsbad, CA). Proteins were separated by SDS-PAGE and transferred to polyvinylidene difluoride membrane (Immobilon transfer membrane; Millipore, Billerica, MA). Membranes were blocked in a buffer of 10 mmol/liter Tris-base, 150 mmol/liter NaCl, and 0.25% Tween 20 containing 7.5% milk for 1 h at room temperature. Membranes were then incubated with primary antibodies overnight at 4 C, followed by incubation with an appropriate horseradish peroxidase-conjugated secondary antibody (Bio-Rad Laboratories, Hercules, CA) for 1 h at room temperature. Bands were visualized using enhanced chemiluminescence (GE Healthcare Europe GmbH, Germany). Immunoreactive proteins were quantified using densitometry.

RNA extraction and gene expression analysis

mRNA expression was assessed in liver from 4-h-fasted mice using quantitative RT-PCR (ABI PRISM 7000 sequence detector system; Applied Biosystems, Foster City, CA). Total RNA was purified from liver using Trizol reagent (Invitrogen). RNA was treated with deoxyribonuclease I using a DNA-free kit (Ambion, Huntingdon, UK), and cDNA was synthesized using a SuperScript first-strand synthesis system (Invitrogen). TaqMan gene expression assays from Applied Biosystems for *Pck-1*; (Mm00440636_m1), *G6pc*; (Mm00839363_m1), and *Scd-1* (Mm00772290_m1) were used with glyceraldehyde-3-phosphate dehydrogenase (*Gapdh*) as a reference gene. The mRNA expression was calculated using the ΔC_t method as described by Applied Biosystems.

Glycogen and triglyceride analyses

A separate cohort of female mice was fasted for 4 h. Mice were anesthetized with sodium pentobarbital, and liver was rapidly removed and frozen in liquid nitrogen. Glycogen content was determined fluorometrically on HCl extracts as previously described (27). Triglycerides were analyzed in pulverized frozen liver. Tissue was homogenized in 300 μl heptan-isopropanol-Tween mixture (3:2:0.01 by volume) and centrifuged (1500 × g for 15 min at 4 C). Supernatants (upper phase containing extracted triglycerides) were collected and evaporated by vacuum centrifugation. Triglyceride content was determined with a triglycerides/glycerol blanked kit (Roche, Basel, Switzerland) using Seronorm lipid (Sero AS, Billingstad, Norway) as a standard.

Reagents and antibodies

Insulin Actrapid was from Novo Nordisk (Bagsværd, Denmark). Horseradish peroxidase-conjugated goat antirabbit and antimouse IgG was obtained from Bio-Rad Laboratories. Reagents for enhanced chemiluminescence were obtained from GE Healthcare. Bicinchoninic acid protein assay kit was from Pierce. All other reagents were of analytical grade (Sigma-Aldrich, St. Louis, MO). Rabbit polyclonal antibodies to glyceraldehyde-3-phosphate dehydrogenase, Akt, glycogen synthase kinase (GSK)-3α/β, IRS-1, phospho-Akt-Ser473, and phospho-GSK-3α/β-Ser21/Ser9 were from Cell Signaling Technology, Inc. (Beverly, MA). Monoclonal 4G10 phosphotyrosine and insulin receptor antibodies and polyclonal IRS-1 and IRS-2 antibodies were from Millipore. Phosphoenolpyruvate carboxykinase 1 (PEPCK) antibody was from Santa Cruz Biotechnology, Inc. (Santa Cruz, CA). The IRS-1-Tyr612 antibody was from Invitrogen. The glu-

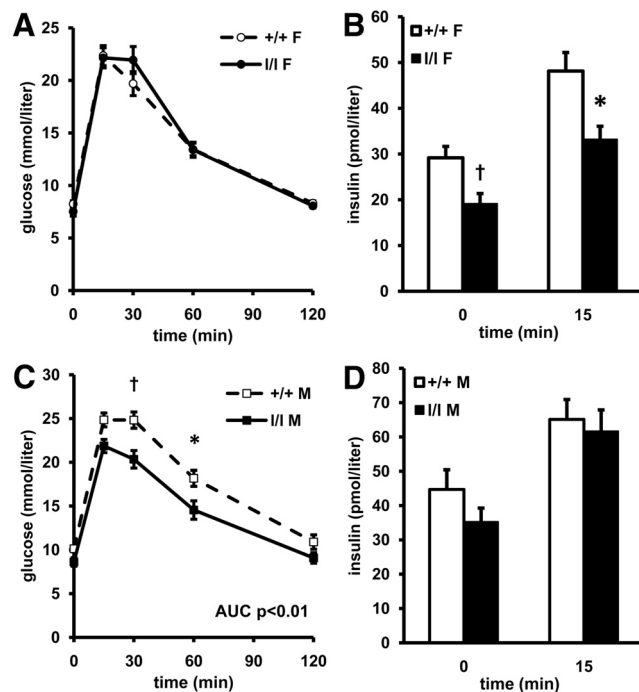


FIG. 1. Glucose homeostasis in *l/l* mice. Intraperitoneal glucose tolerance tests were performed in 4-h-fasted +/+ (white bars) and *l/l* (black bars) mice. Plasma glucose (mmol/liter) and insulin (pmol/liter) were analyzed during the glucose tolerance test in female (F; A and B) and male (M; C and D) +/+ and *l/l* mice. Results are mean ± SEM. *, $P < 0.05$ vs. +/+; †, $P < 0.01$ vs. +/+ mice ($n = 9-12$).

cose transporter 4 antibody was a kind gift from Professor Geoffrey Holman (University of Bath, Bath, UK).

Statistics

Statistical differences were determined by a two-way ANOVA with multiple comparisons. Student's *t* test was used for comparisons when two parameters were evaluated. Significance was accepted at $P < 0.05$.

Results

Glucose homeostasis in *l/l* mice

We have previously shown that the blood glucose concentration under *ad libitum*-fed conditions is normal in female and male *l/l* mice. Conversely, insulin level is reduced 40% in female *l/l* mice and unaltered in male *l/l* mice (24). We determined ip glucose tolerance in *+/+* and *l/l* mice. Fasting glucose levels were normal in female and male *l/l* mice compared with age-matched *+/+* mice (Fig. 1, A and C). The glucose profile over 2 h was similar between female *+/+* and *l/l* mice (Fig. 1A). However, insulin concentration was reduced at baseline ($P < 0.05$) and 15 min ($P < 0.01$) after the glucose injection (Fig. 1B), which indicates insulin sensitivity is enhanced in female *l/l* mice compared with *+/+* mice. Interestingly, male *l/l* mice have an improved glucose tolerance. The area under the glucose curve is reduced in male *l/l* compared with *+/+* mice (*+/+*, 2152 ± 80 vs. *l/l*, 1778 ± 88 ; $P < 0.01$). The insulin levels are, however, unaltered both at baseline and 15 min after the glucose injection in male *l/l* mice (Fig. 1D).

In vitro glucose transport and insulin signaling in skeletal muscle

Insulin-stimulated glucose transport was assessed in isolated skeletal muscle from *+/+* and *l/l* mice. Isolated EDL and soleus muscles were incubated *in vitro* without or with 0.36 and 60 nmol/liter insulin. Basal and insulin-stimulated glucose transport in isolated EDL and soleus muscle was similar between female *+/+* and *l/l* mice (Fig. 2, A and B). Despite the improved glucose tolerance observed in the male *l/l* mice, *in vitro* insulin-stimulated glucose transport was similar in male *+/+* and *l/l* mice (Supplemental Fig. 1, A and B, published on The Endocrine Society's Journals Online web site at <http://endo.endo-journals.org>). Consistently, protein expression of the insulin-responsive glucose transporter 4 in EDL and soleus muscle was similar between *+/+* and *l/l* mice (data not

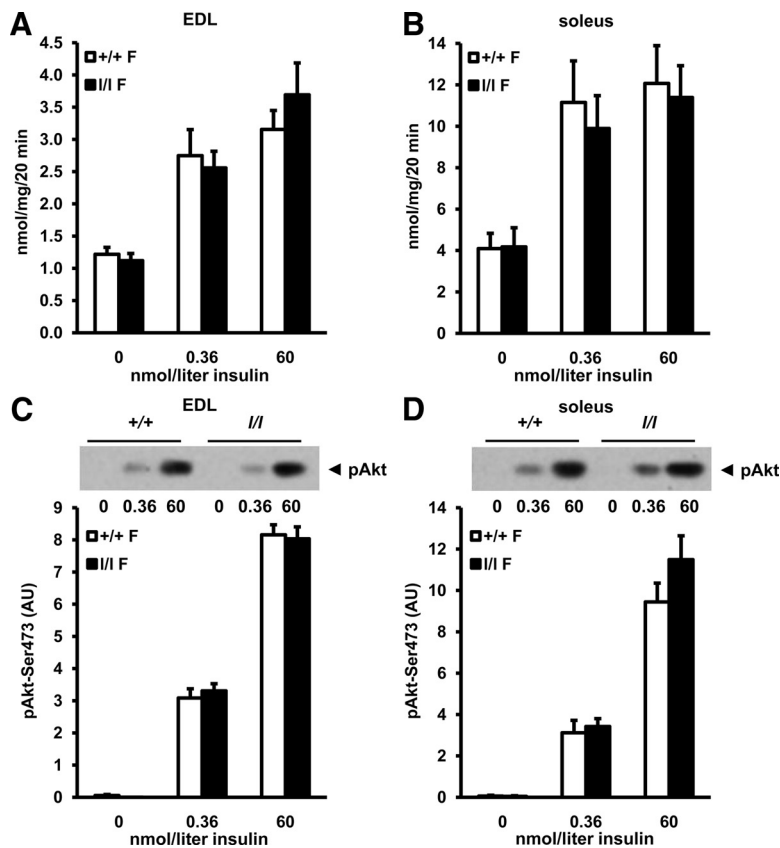


FIG. 2. Insulin-stimulated glucose transport in isolated skeletal muscle. Isolated EDL and soleus muscle from 4-h-fasted female *+/+* and *l/l* mice was incubated *in vitro* without and with 0.36 and 60 nmol/liter insulin. Basal and insulin-stimulated *in vitro* glucose transport in isolated EDL (A) and soleus (B) muscle from *+/+* (white bars) and *l/l* (black bars) mice. Basal and insulin-stimulated Akt-Ser473 phosphorylation in isolated EDL (C) and soleus (D) muscle from female (F) *+/+* (white bars) and *l/l* (black bars) mice. Results are mean \pm SEM ($n = 6-9$).

shown). Moreover, basal and insulin-stimulated phosphorylation of Akt-Ser473, a key component in the canonical insulin signaling pathway controlling glucose uptake, was similar in EDL and soleus muscle from female *+/+* and *l/l* mice (Fig. 2, C and D).

Whole-body insulin sensitivity

We performed a euglycemic-hyperinsulinemic clamp study, whereby insulin was infused into conscious mice to assess peripheral glucose utilization and hepatic glucose production. The glucose turnover rate was similar in female and male *+/+* and *l/l* mice in the basal state (Fig. 3, A and C). Both female and male *l/l* mice had a reduced body weight compared with *+/+* mice, and the clamps were performed at similar glucose and insulin concentrations (Table 1). In the female mice, the insulin infusion (1.25 mU/kg \cdot min) increased plasma insulin levels approximately 2.5-fold. Insulin infusion increased peripheral glucose utilization approximately 1.8-fold in both *+/+* and *l/l* mice ($P < 0.01$). Furthermore, the insulin infusion reduced hepatic glucose production 46% in the

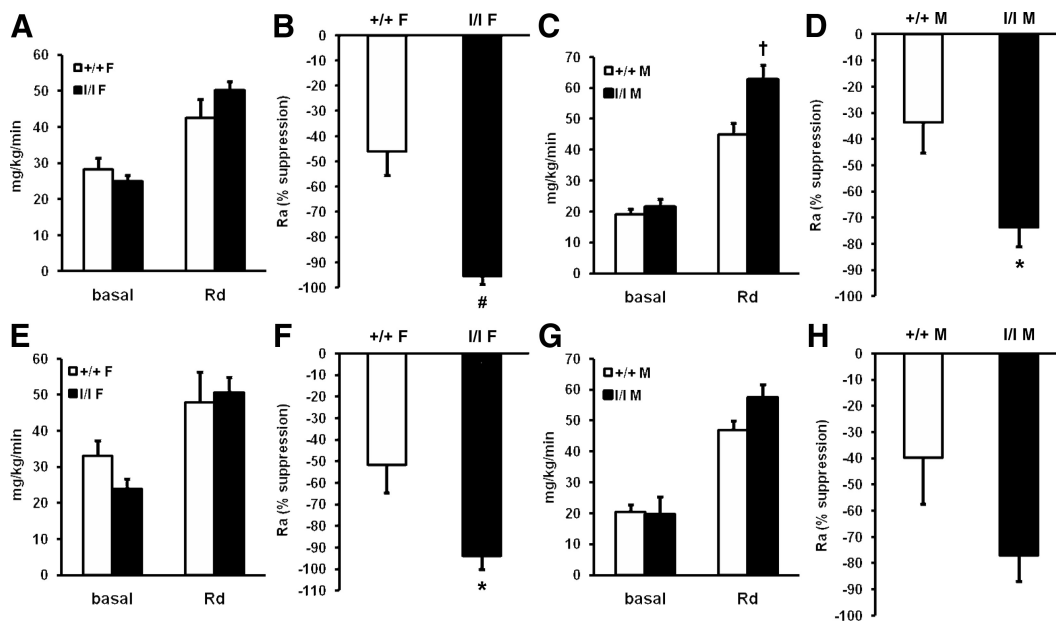


FIG. 3. Whole-body glucose utilization in conscious mice. Basal and insulin-stimulated (Rd) peripheral glucose utilization and hepatic glucose production (Ra) were determined during a euglycemic-hyperinsulinemic clamp in 4-h-fasted *+/+* (white bars) and *l/l* (black bars) mice. Glucose utilization and the insulin-mediated suppression of hepatic glucose production are presented for female (F; A and B) and male (M; C and D) *+/+* and *l/l* mice ($n = 7-9$). E-H, A subset of body weight-matched *+/+* and *l/l* mice. Glucose utilization and insulin-mediated suppression of hepatic glucose production are presented for female (E and F) and male (G and H) *+/+* and *l/l* mice ($n = 4-5$). Results are mean \pm SEM. *, $P < 0.05$, †, $P < 0.01$, and #, $P < 0.001$ vs. *+/+* mice.

liver from female *+/+* mice (Fig. 3B). In the *l/l* mice, insulin-induced suppression of hepatic glucose production was markedly increased (Fig. 3B; $P < 0.001$). Hepatic glucose production was completely suppressed in the *l/l* mice. Thus, hepatic insulin sensitivity is enhanced in female *l/l* mice. The male *l/l* mice also display enhanced hepatic insulin sensitivity. An insulin infusion (2.5 mU/kg \cdot min) suppressed hepatic glucose production 74% in male *l/l* mice compared with 34% in *+/+* mice (Fig. 3D; $P < 0.05$). Furthermore, the male *l/l* mice show an increased insulin-stimulated glucose utilization compared with *+/+* mice (Fig. 3C; $P < 0.01$). Enhanced insulin sensitivity is supported by the increased steady-state glucose

infusion rate under the clamp observed in female and male *l/l* mice compared with respective *+/+* mice (Table 1; $P < 0.001$). We further report glucose utilization and hepatic glucose production in a subset of body weight-matched female and male *+/+* and *l/l* mice. Insulin suppression of hepatic glucose production is increased (Fig. 3E; $P < 0.05$) in female *l/l* mice compared with body weight-matched *+/+* mice (body weight: *+/+*, 19.7 ± 0.8 g vs. *l/l*, 19.3 ± 0.5 g). Basal and insulin-stimulated glucose utilization is similar in female *+/+* and *l/l* mice (Fig. 3F). In the body weight-matched male *+/+* and *l/l* mice (body weight; *+/+*, 28.0 ± 0.2 g vs. *l/l*, 27.3 ± 0.3 g), basal glucose utilization is unaltered (Fig. 3G). There is a trend for in-

TABLE 1. Basal and clamp characteristics in female and male *+/+* and *l/l* mice

	Female		Male	
	<i>+/+</i>	<i>l/l</i>	<i>+/+</i>	<i>l/l</i>
Body weight (g)	20.6 ± 0.5	18.4 ± 0.4^a	28.5 ± 0.2	26.6 ± 0.4^a
Basal				
Plasma glucose (mmol/liter)	8.1 ± 0.7	6.5 ± 0.4	9.0 ± 0.4	8.5 ± 0.6
Plasma insulin (pmol/liter)	86.9 ± 14.1	52.2 ± 6.3^b	141.3 ± 21.3	102.8 ± 18.8
Clamp				
Plasma glucose (mmol/liter)	6.8 ± 0.5	6.3 ± 0.5	8.6 ± 0.2	8.8 ± 0.4
Plasma insulin (pmol/liter)	191.7 ± 14.1	145.6 ± 13.8	516.7 ± 31.2	471.5 ± 27.0
Glucose infusion rate (mg/kg \cdot min)	28.6 ± 5.0	50.0 ± 1.3^c	30.8 ± 3.6	56.2 ± 3.8^c

Results are mean \pm SEM ($n = 6-10$).

^a $P < 0.01$ vs. *+/+*.

^b $P < 0.05$ vs. *+/+*.

^c $P < 0.001$ vs. *+/+*.

TABLE 2. Blood chemistry in 4-h-fasted +/+ and *l/l* mice

	Female		Male	
	+/+	<i>l/l</i>	+/+	<i>l/l</i>
Insulin (pmol/liter)	48.5 ± 2.5	31.9 ± 2.7 ^a	55.0 ± 6.4	52.0 ± 8.0
Leptin (ng/ml)	0.59 ± 0.11	0.22 ± 0.08 ^b	0.94 ± 0.21	0.43 ± 0.11 ^b
Resistin (ng/ml)	1.67 ± 0.08	1.59 ± 0.03	1.41 ± 0.06	1.43 ± 0.05
PAI-1 (ng/ml)	2.43 ± 0.33	2.32 ± 0.40	1.94 ± 0.28	2.64 ± 0.34
Adiponectin (μg/ml)	10.8 ± 0.4	11.7 ± 0.6		

Results are mean ± SEM (n = 5–12).

^a *P* < 0.001 vs. +/+.

^b *P* < 0.05 vs. +/+.

creased insulin-stimulated glucose utilization and the suppression of hepatic glucose production in male *l/l* mice (Fig. 3, G and H), which did not reach statistical significance in this subset of animals.

Blood chemistry

Blood was collected from 4-h-fasted female and male +/+ and *l/l* mice. Serum leptin concentrations were reduced in female and male *l/l* mice, and insulin concentrations were reduced in female *l/l* mice but unchanged in male *l/l* mice (Table 2), consistent with our previous observations (24). tPAI-1 and resistin were unchanged in female and male *l/l* mice. Serum adiponectin levels were also unaltered between female +/+ and *l/l* mice.

Signal transduction in the liver

We determined insulin signaling in liver of +/+ and *l/l* mice. Liver was collected after approximately 75 min of insulin infusion during the clamp from male +/+ and *l/l* mice. Insulin-stimulated tyrosine phosphorylation of insulin receptor in liver tended to be increased in male *l/l* mice compared with +/+ mice (Fig. 4A; *P* = 0.07). Protein expression of the insulin receptor was, however, similar in male +/+ and *l/l* mice (Fig. 4A). Insulin-stimulated tyrosine phosphorylation and protein expression of IRS-1 and IRS-2 were similar in male +/+ and *l/l* mice after the clamp (Fig. 4, B and C). Insulin-stimulated Akt-Ser473 phosphorylation and protein expression were also unaltered between male +/+ and *l/l* mice (Fig. 4D). Similarly, tyrosine phosphorylation of insulin receptor, IRS-1, and IRS-2 and phosphorylation of Akt-Ser473 were not altered in female *l/l* mice after a 10-min insulin infusion (Supplemental Fig. 2). We further determined insulin receptor and IRS-1 tyrosine phosphorylation and Akt-Ser473 phosphorylation 10 min after a saline or insulin injection (0.1 mU/g; ip). Basal and insulin-stimulated insulin receptor and IRS-1 tyrosine phosphorylation were unaltered in liver from female *l/l* mice (Fig. 5, A and B). Phosphorylation of IRS-1 at Tyr612 and Akt-Ser473 was also unchanged in female (Fig. 5, C and D) and male

(Supplemental Fig. 3, A and B) *l/l* mice, with the exception of a reduction in Akt-Ser473 phosphorylation in liver from female *l/l* mice after saline injection (Fig. 5D; *P* < 0.05). Protein expression of components of the early canonical insulin signaling pathway, including the insulin receptor, IRS-1, and IRS-2, were similar between female +/+ and *l/l* mice (Supplemental Fig. 4). In addition, a low dose of insulin was injected ip and liver was removed after 10 min for determination of Akt-Ser473 phosphorylation. Insulin increased Akt-Ser473 phosphorylation 2-fold in +/+ mice (data not shown). Insulin-stimulated Akt-Ser473 phosphorylation was unaltered between +/+ and *l/l* mice (Supplemental Fig. 3C). Moreover, basal phosphorylation of GSK3α at Ser21 was similar between +/+ and *l/l* mice (Supplemental Fig. 3D). Protein expression of Akt and GSK3α were unchanged between female +/+ and *l/l* mice (Supplemental Fig. 3, C and D).

Liver composition and expression profile

A separate cohort of female mice was used to assess liver glycogen and triglyceride content and gene expression. Liver glycogen and triglycerides content in 4-h-fasted mice was similar between +/+ and *l/l* mice (Table 3). In addition, hepatic gene expression of the gluconeogenic enzymes *Pck-1* and *G6Pc* was unaltered between +/+ and *l/l* mice (Table 3). We also determined PEPCCK protein expression, which in accordance with the RNA expression data, was unaltered between +/+ and *l/l* mice (data not shown). Although the RNA expression of *Scd-1* was significantly increased in liver from *l/l* vs. +/+ mice (data not shown), SCD-1 protein expression was unaltered (+/+, 5.3 ± 0.2 vs. *l/l*, 5.2 ± 0.3; Supplemental Fig. 5C).

Liver mitochondrial respiratory control in *l/l* mice

We assessed mitochondrial function in mechanically permeabilized liver from female +/+ and *l/l* mice using high-resolution respirometry to measure electron transfer and respiratory control through complex I (by adding

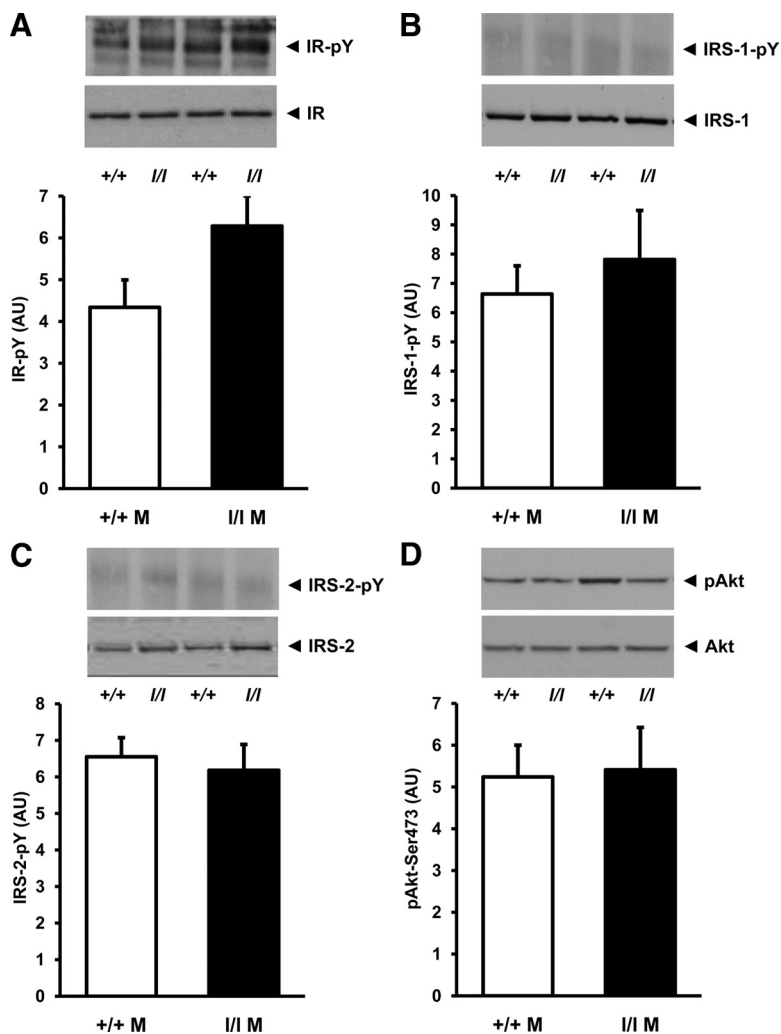


FIG. 4. Insulin signaling in liver after a euglycemic-hyperinsulinemic clamp. Tyrosine phosphorylation of insulin receptor (IR) (A), IRS-1 (B), and IRS-2 (C) and phosphorylation of Akt-Ser473 (D) were determined in liver for male (M) *+/+* (white bars) and *l/l* (black bars) mice after a clamp (2.5 mU/kg · min insulin infusion). Representative blots show phosphorylated proteins (top panel) and protein expression (bottom panel). Results are mean \pm SEM (n = 6–8).

malate, glutamate and pyruvate) and/or complex II (by supplying succinate). Excess ADP was added to assess electron transfer coupled to oxidative phosphorylation. The mitochondrial uncoupler protonophore carbonylcyanide-4-(trifluoromethoxy)-phenylhydrazone was added to reach the maximal capacity of the electron transfer system. Oxygen flux normalized to liver wet weight (Supplemental Fig. 5A) and flux control ratios (Supplemental Fig. 5B) were similar between *+/+* and *l/l* mice. We also determined the protein content of several markers of the oxidative phosphorylation system, succinate-ubiquinol oxidoreductase 70-kDa subunit (complex II), cytochrome oxidase subunit I (complex IV), and ATP synthase subunit- α . Consistent with our functional data, the mitochondrial protein content was similar between *+/+* and *l/l* mice (Supplemental Fig. 5C).

Discussion

The absence of leptin or LepRb in *ob/ob* and *db/db* mice leads to the development of insulin resistance and type 2 diabetes. Leptin regulates glucose homeostasis indirectly, by regulating adipose tissue mass, and directly, by acting on hepatic and peripheral tissues. By using mouse models with leptin receptor mutations that block specific leptin receptor signaling pathways, we determined pathways important for the regulation of glucose metabolism. Glucose homeostasis is improved in LepRb-Tyr1138 mutant mice lacking the LepRb-STAT3 pathway, compared with *db/db* mice via a mechanism involving adiposity-dependent and -independent signals (19). The physiological importance of signals from the LepRb-Tyr1077/STAT5 pathway, as well as signals mediated directly by LepRb-associated Jak2 pathway, in the control of glucose homeostasis is unknown.

We studied female and male *l/l* mice with mutant leptin receptors at LepRb-Tyr985 to assess the physiological role of the LepRb-SHP2/SOCS3 pathway in glucose homeostasis (24). The mutant LepRb-Tyr985 receptor blocks the binding of SOCS3 to the receptor. SOCS3 is induced by leptin and acts as a negative regulator of leptin receptor signaling, thereby promoting leptin resistance (23, 28). We previously reported that female *l/l* mice have reduced body weight due to a reduced adiposity, whereas male *l/l* mice have a normal body weight at 12 wk of age. Circulating leptin concentrations are appropriately reduced in female *l/l* mice. Although the body weight of male *l/l* mice is normal at 12 wk of age, leptin levels are reduced at 8 wk of age, suggesting a modest effect of Tyr985 mutation on adiposity also in the male *l/l* mice (24). We now report that at 15–17 wk of age, male *l/l* mice also have reduced body weight. Although glucose tolerance is normal in female *l/l* mice, the reduced insulin concentrations in either the fed or the fasted state in these mice indicate insulin sensitivity is enhanced. Male *l/l* mice, on the other hand, show improved glucose tolerance with unaltered insulin concentrations at baseline and 15 min after the glucose injection. Although leptin levels are reduced in *l/l* mice (24), adiponectin, resistin, and tPAI-1 are unaltered. Mice with heterozygous SOCS3 deficiency are lean and leptin sensitive, similar to the *l/l* mice. Furthermore, SOCS3 heterozygous mice are protected against development of diet-induced obesity and insulin resistance

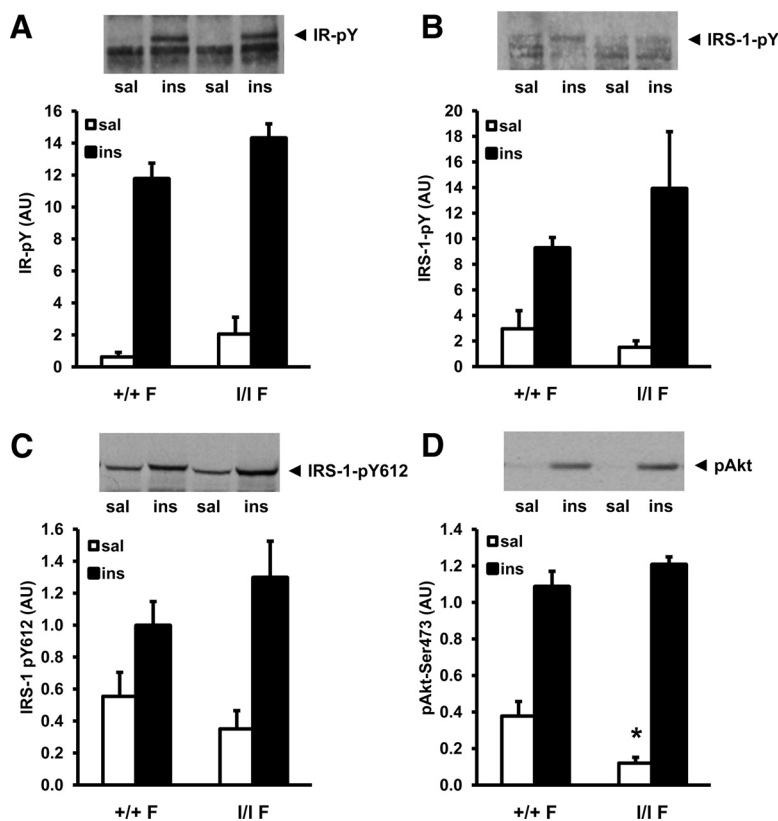


FIG. 5. Liver signaling. Female (F) $+/+$ and l/l mice were fasted for 4 h and then injected with saline (white bars) or insulin (black bars) (0.1 mU/g, ip). Liver was collected after 10 min. Tyrosine phosphorylation of insulin receptor (IR) (A), IRS-1 (B), IRS-1-Tyr612 (C), and phosphorylation of Akt-Ser473 (D) were determined. Representative blots show phosphorylated proteins. Results are mean \pm SEM. *, $P < 0.05$ vs. $+/+$ mice ($n = 3-6$).

(29, 30). Selective deletion of SOCS3 in proopiomelanocortin-expressing cells results in enhanced leptin sensitivity. On a chow diet, glucose homeostasis was improved despite no change in body weight (31). Previous reports also show that mice with a neuronal disruption of SHP2 are obese and leptin and insulin resistant (32, 33), suggesting that lack of SOCS3 and not SHP2 is responsible for the improved insulin sensitivity in l/l mice.

Using the gold standard for analyzing insulin sensitivity, the euglycemic-hyperinsulinemic clamp, we provide

TABLE 3. Liver substrates and gene expression in female $+/+$ and l/l mice

	$+/+$	l/l
Glycogen (mg/g tissue)	25.0 \pm 3.0	24.8 \pm 1.7
Triglycerides (mg/g tissue)	14.3 \pm 0.5	15.7 \pm 0.7
<i>Pck-1</i> (arbitrary units)	2.52 \pm 0.23	2.71 \pm 0.27
<i>G6pc</i> (arbitrary units)	1.35 \pm 0.21	1.47 \pm 0.29

Results are mean \pm SEM ($n = 8-12$).

evidence that whole-body glucose utilization is unaltered between female and male $+/+$ and l/l mice under basal conditions. Although insulin-stimulated glucose utilization is normal in female l/l mice, it is enhanced in the male l/l mice. The improved whole-body glucose utilization in male l/l mice is further supported by the improved glucose tolerance. However, basal and insulin-stimulated glucose transport in isolated skeletal muscle is similar between $+/+$ and l/l mice. Hepatic insulin sensitivity is enhanced in both female and male l/l mice because insulin-induced suppression of glucose production was increased, indicating inhibitory leptin signals are important for insulin sensitivity in liver. To explore the possible influence of reduced adiposity on glucose utilization and hepatic glucose production, data from a subset of body weight-matched $+/+$ and l/l mice were examined and revealed similar results. Thus, the enhanced insulin sensitivity observed in the LepRb-Tyr985 mutant mice is predominantly primary and not due to changes in body weight.

The liver plays an important role in the regulation of glucose metabolism. Glucose production from the liver can be controlled from two simultaneous ongoing pathways. Glucose is produced by the breakdown of glycogen (glycogenolysis) and by *de novo* synthesis of glucose (gluconeogenesis) from precursors such as lactate, amino acids, and glycerol. The contributions of these pathways for glucose production varies, depending on the metabolic and nutritional state (34) and may not be similar in $+/+$ and l/l mice. Because the suppression of hepatic glucose production by insulin is markedly improved in l/l mice, we determined whether changes in glycogen and triglyceride levels were altered. However, liver glycogen and triglyceride content was similar between female $+/+$ and l/l mice. Thus, the enhanced hepatic insulin sensitivity is likely to account for the reduction in insulin levels during the glucose tolerance test in the female l/l mice.

The hypothalamus plays a key role in the regulation of hepatic glucose production (9, 10). In rats, an acute administration of leptin enhances the effect of insulin to inhibit glucose production (7). Furthermore, restoration of hypothalamic leptin action in leptin receptor-deficient Koltzky rats improves hepatic insulin sensitivity by enhancing the suppression of glucose production (35). The mechanism by which hepatic insulin sensitivity is enhanced in l/l mice is still unclear. Improved leptin sensitivity, as observed in the female l/l mice, could explain the reduction

in hepatic glucose production. If this effect is centrally mediated or is due to direct effects of leptin in the liver remains to be determined.

To explore the mechanism mediating the enhanced hepatic insulin sensitivity in *l/l* mice, early insulin signaling and expression of key genes were assessed. However, expression of the gluconeogenic enzymes PEPCCK and glucose-6-phosphatase and protein expression and activation of several early components of the insulin signaling pathway, including the insulin receptor, IRS-1, and IRS-2, were unaltered between *+/+* and *l/l* mice. This is in contrast to *db/db* mice that lack the leptin receptor and *s/s* mice that lack the LepRb-STAT3 pathway because both of these models have a pronounced reduction of IRS-2 expression in the liver (19). Furthermore, *db/db* and *s/s* mice also have an increased expression of stearoyl-coenzyme A desaturase 1 (SCD-1) in the liver. SCD-1 catalyzes the synthesis of monounsaturated fatty acids and is regulated by leptin in the liver (36). Insulin sensitivity is enhanced in whole-body SCD-1 knockout mice, partly due to reduced adiposity (37). Although we report that liver *Scd-1* mRNA expression in female *l/l* mice is increased 2-fold, SCD-1 protein content was unaltered and thus unlikely to play a role in insulin sensitivity in *l/l* mice.

Enhanced mitochondrial respiration may also provide a potential link between hepatic mitochondrial function and insulin sensitivity. Defective hepatic mitochondrial function in leptin deficient *ob/ob* mice is improved by leptin treatment (38). However, female *l/l* mice have normal mitochondrial function and protein expression of key mitochondrial proteins such as succinate-ubiquinol oxidoreductase 70 kDa subunit, ATP synthase- α , and cytochrome oxidase subunit I, indicating the enhanced hepatic insulin sensitivity may be related to increased parasympathetic nervous system activity, rather than liver-specific changes in metabolic gene reprogramming.

In addition, changes in glucagon response (39) could also influence hepatic glucose production. Furthermore, direct intracerebral infusion of nutrients, as well as insulin and leptin, has been shown to decrease hepatic glucose production (40–42). Taken together, given the unaltered insulin signaling noted in livers from *l/l* mice, extrahepatic mechanisms, possibly at the level of the hypothalamus, may explain the reduction in hepatic glucose production. Thus, further studies are warranted to address whether altered hypothalamic insulin signaling in *l/l* mice alters hepatic tone and insulin suppression of glucose production.

In conclusion, we report that signals emanating from the leptin receptor control hepatic insulin sensitivity in female and male mice. Male mice lacking the LepRb-Tyr985 pathway also display improved peripheral glucose

utilization. Lack of the LepRb-Tyr985 recruitment of SHP2/SOCS3 enhances whole-body insulin sensitivity through increased insulin action on the suppression of hepatic glucose production. Central leptin and insulin action might contribute to the phenotype, but this remains to be established.

Acknowledgments

We thank Professor Juleen R. Zierath, Marc Gilbert, and Anna Krook for helpful discussions and critical reading of the manuscript.

Address all correspondence and requests for reprints to: Marie Björnholm, Integrative Physiology, Department of Molecular Medicine and Surgery, Karolinska Institutet, von Eulers väg 4a, IV, SE-171 77, Stockholm, Sweden. E-mail: marie.bjornholm@ki.se.

This work was supported by grants from the Swedish Research Council, the Novo Nordisk Foundation, and the European Foundation for the Study of Diabetes/Lilly Research Fellowship, the Karolinska Institutet, the Knut and Alice Wallenberg Foundation (2005.0120), the FoUU Karolinska University Hospital, the Swedish Diabetes Association, the Swedish Society of Medicine, the Magnus Bergvall Foundation, the Åke Wiberg Foundation, the Sigurd och Elsa Golje Foundation, the Lars Hierta Memorial Foundation, the Jeansson Foundation, the O. E. and Edla Johansson Foundation, and the Fredrik and Ingrid Thuring Foundation. Present address for E.I.-G.: Department of Pharmaceutical and Food Sciences, CEU San Pablo University, Madrid 28668, Spain.

Disclosure Summary: The authors have nothing to disclose.

References

- Zhang Y, Proenca R, Maffei M, Barone M, Leopold L, Friedman JM 1994 Positional cloning of the mouse obese gene and its human homologue. *Nature* 372:425–432
- Tartaglia LA, Dembski M, Weng X, Deng N, Culpepper J, Devos R, Richards GJ, Campfield LA, Clark FT, Deeds J, Muir C, Sanker S, Moriarty A, Moore KJ, Smutko JS, Mays GG, Wool EA, Monroe CA, Tepper RI 1995 Identification and expression cloning of a leptin receptor, OB-R. *Cell* 83:1263–1271
- Chua Jr SC, Koutras IK, Han L, Liu SM, Kay J, Young SJ, Chung WK, Leibel RL 1997 Fine structure of the murine leptin receptor gene: splice site suppression is required to form two alternatively spliced transcripts. *Genomics* 45:264–270
- Friedman JM, Halaas JL 1998 Leptin and the regulation of body weight in mammals. *Nature* 395:763–770
- Farooqi IS, O'Rahilly S 2009 Leptin: a pivotal regulator of human energy homeostasis. *Am J Clin Nutr* 89:980S–984S
- Kamohara S, Burcelin R, Halaas JL, Friedman JM, Charron MJ 1997 Acute stimulation of glucose metabolism in mice by leptin treatment. *Nature* 389:374–377
- Rossetti L, Massillon D, Barzilai N, Vuguin P, Chen W, Hawkins M, Wu J, Wang J 1997 Short term effects of leptin on hepatic gluconeogenesis and *in vivo* insulin action. *J Biol Chem* 272:27758–27763

8. Liu L, Karkanias GB, Morales JC, Hawkins M, Barzilay N, Wang J, Rossetti L 1998 Intracerebroventricular leptin regulates hepatic but not peripheral glucose fluxes. *J Biol Chem* 273:31160–31167
9. Obici S, Zhang BB, Karkanias G, Rossetti L 2002 Hypothalamic insulin signaling is required for inhibition of glucose production. *Nat Med* 8:1376–1382
10. Pocai A, Lam TK, Gutierrez-Juarez R, Obici S, Schwartz GJ, Bryan J, Aguilar-Bryan L, Rossetti L 2005 Hypothalamic KATP channels control hepatic glucose production. *Nature* 434:1026–1031
11. Minokoshi Y, Kim YB, Peroni OD, Fryer LG, Müller C, Carling D, Kahn BB 2002 Leptin stimulates fatty-acid oxidation by activating AMP-activated protein kinase. *Nature* 415:339–343
12. Minokoshi Y, Shiuchi T, Lee S, Suzuki A, Okamoto S 2008 Role of hypothalamic AMP-kinase in food intake regulation. *Nutrition* 24:786–790
13. Ghilardi N, Skoda RC 1997 The leptin receptor activates Janus kinase 2 and signals for proliferation in a factor-dependent cell line. *Mol Endocrinol* 11:393–399
14. Banks AS, Davis SM, Bates SH, Myers Jr MG 2000 Activation of downstream signals by the long form of the leptin receptor. *J Biol Chem* 275:14563–14572
15. Carpenter LR, Farruggella TJ, Symes A, Karow ML, Yancopoulos GD, Stahl N 1998 Enhancing leptin response by preventing SH2-containing phosphatase 2 interaction with Ob receptor. *Proc Natl Acad Sci USA* 95:6061–6066
16. Ghilardi N, Ziegler S, Wiestner A, Stoffel R, Heim MH, Skoda RC 1996 Defective STAT signaling by the leptin receptor in diabetic mice. *Proc Natl Acad Sci USA* 93:6231–6235
17. Bates SH, Stearns WH, Dundon TA, Schubert M, Tso AW, Wang Y, Banks AS, Lavery HJ, Haq AK, Maratos-Flier E, Neel BG, Schwartz MW, Myers Jr MG 2003 STAT3 signaling is required for leptin regulation of energy balance but not reproduction. *Nature* 421:856–859
18. Bates SH, Dundon TA, Seifert M, Carlson M, Maratos-Flier E, Myers Jr MG 2004 LRB-STAT3 signaling is required for the neuroendocrine regulation of energy expenditure by leptin. *Diabetes* 53:3067–3073
19. Bates SH, Kulkarni RN, Seifert M, Myers Jr MG 2005 Roles for leptin receptor/STAT3-dependent and -independent signals in the regulation of glucose homeostasis. *Cell Metab* 1:169–178
20. Gong Y, Ishida-Takahashi R, Villanueva EC, Fingar DC, Münzberg H, Myers Jr MG 2007 The long form of the leptin receptor regulates STAT5 and ribosomal protein S6 via alternate mechanisms. *J Biol Chem* 282:31019–31027
21. Ren D, Li M, Duan C, Rui L 2005 Identification of SH2-B as a key regulator of leptin sensitivity, energy balance, and body weight in mice. *Cell Metab* 2:95–104
22. Feener EP, Rosario F, Dunn SL, Stancheva Z, Myers Jr MG 2004 Tyrosine phosphorylation of Jak2 in the JH2 domain inhibits cytokine signaling. *Mol Cell Biol* 24:4968–4978
23. Bjørbaek C, Lavery HJ, Bates SH, Olson RK, Davis SM, Flier JS, Myers Jr MG 2000 SOCS3 mediates feedback inhibition of the leptin receptor via Tyr985. *J Biol Chem* 275:40649–40657
24. Bjørnholm M, Münzberg H, Leshan RL, Villanueva EC, Bates SH, Louis GW, Jones JC, Ishida-Takahashi R, Bjørbaek C, Myers Jr MG 2007 Mice lacking inhibitory leptin receptor signals are lean with normal endocrine function. *J Clin Invest* 117:1354–1360
25. Barnes BR, Marklund S, Steiler TL, Walter M, Hjalms G, Amarger V, Mahlapuu M, Leng Y, Johansson C, Galuska D, Lindgren K, Abrink M, Stapleton D, Zierath JR, Andersson L 2004 The 5'-AMP-activated protein kinase γ 3 isoform has a key role in carbohydrate and lipid metabolism in glycolytic skeletal muscle. *J Biol Chem* 279:38441–38447
26. Chibalin AV, Leng Y, Vieira E, Krook A, Bjørnholm M, Long YC, Kotova O, Zhong Z, Sakane F, Steiler T, Nylén C, Wang J, Laakso M, Topham MK, Gilbert M, Wallberg-Henriksson H, Zierath JR 2008 Downregulation of diacylglycerol kinase Δ contributes to hyperglycemia-induced insulin resistance. *Cell* 132:375–386
27. Long YC, Barnes BR, Mahlapuu M, Steiler TL, Martinsson S, Leng Y, Wallberg-Henriksson H, Andersson L, Zierath JR 2005 Role of AMP-activated protein kinase in the coordinated expression of genes controlling glucose and lipid metabolism in mouse white skeletal muscle. *Diabetologia* 48:2354–2364
28. Münzberg H, Myers Jr MG 2005 Molecular and anatomical determinants of central leptin resistance. *Nat Neurosci* 8:566–570
29. Mori H, Hanada R, Hanada T, Aki D, Mashima R, Nishinakamura H, Torisu T, Chien KR, Yasukawa H, Yoshimura A 2004 Socs3 deficiency in the brain elevates leptin sensitivity and confers resistance to diet-induced obesity. *Nat Med* 10:739–743
30. Howard JK, Cave BJ, Oksanen LJ, Tzamelis I, Bjørbaek C, Flier JS 2004 Enhanced leptin sensitivity and attenuation of diet-induced obesity in mice with haploinsufficiency of Socs3. *Nat Med* 10:734–738
31. Kievit P, Howard JK, Badman MK, Balthasar N, Coppari R, Mori H, Lee CE, Elmquist JK, Yoshimura A, Flier JS 2006 Enhanced leptin sensitivity and improved glucose homeostasis in mice lacking suppressor of cytokine signaling-3 in POMC-expressing cells. *Cell Metab* 4:123–132
32. Banno R, Zimmer D, De Jonghe BC, Atienza M, Rak K, Yang W, Bence KK 2010 PTP1B and SHP2 in POMC neurons reciprocally regulate energy balance in mice. *J Clin Invest* 120:720–734
33. Zhang EE, Chapeau E, Hagihara K, Feng GS 2004 Neuronal Shp2 tyrosine phosphatase controls energy balance and metabolism. *Proc Natl Acad Sci USA* 101:16064–16069
34. Burgess SC, Jeffrey FM, Storey C, Milde A, Hausler N, Merritt ME, Mulder H, Holm C, Sherry AD, Malloy CR 2005 Effect of murine strain on metabolic pathways of glucose production after brief or prolonged fasting. *Am J Physiol Endocrinol Metab* 289:E53–E61
35. German J, Kim F, Schwartz GJ, Havel PJ, Rhodes CJ, Schwartz MW, Morton GJ 2009 Hypothalamic leptin signaling regulates hepatic insulin sensitivity via a neurocircuit involving the vagus nerve. *Endocrinology* 150:4502–4511
36. Cohen P, Miyazaki M, Succi ND, Hagge-Greenberg A, Liedtke W, Soukas AA, Sharma R, Hudgins LC, Ntambi JM, Friedman JM 2002 Role for stearyl-CoA desaturase-1 in leptin-mediated weight loss. *Science* 297:240–243
37. Ntambi JM, Miyazaki M, Stoehr JP, Lan H, Kendzierski CM, Yandell BS, Song Y, Cohen P, Friedman JM, Attie AD 2002 Loss of stearyl-CoA desaturase-1 function protects mice against adiposity. *Proc Natl Acad Sci USA* 99:11482–11486
38. Singh A, Wirtz M, Parker N, Hogan M, Strahler J, Michailidis G, Schmidt S, Vidal-Puig A, Diano S, Andrews P, Brand MD, Friedman J 2009 Leptin-mediated changes in hepatic mitochondrial metabolism, structure, and protein levels. *Proc Natl Acad Sci USA* 106:13100–13105
39. Berglund ED, Lee-Young RS, Lustig DG, Lynes SE, Donahue EP, Camacho RC, Meredith ME, Magnuson MA, Charron MJ, Wasserman DH 2009 Hepatic energy state is regulated by glucagon receptor signaling in mice. *J Clin Invest* 119:2412–2422
40. Lam TK, Gutierrez-Juarez R, Pocai A, Rossetti L 2005 Regulation of blood glucose by hypothalamic pyruvate metabolism. *Science* 309:943–947
41. Obici S, Feng Z, Morgan K, Stein D, Karkanias G, Rossetti L 2002 Central administration of oleic acid inhibits glucose production and food intake. *Diabetes* 51:271–275
42. Pocai A, Morgan K, Buettner C, Gutierrez-Juarez R, Obici S, Rossetti L 2005 Central leptin acutely reverses diet-induced hepatic insulin resistance. *Diabetes* 54:3182–3189